NANO LETTERS

Letter

pubs.acs.org/NanoLett

Ripping Graphene: Preferred Directions

Kwanpyo Kim,[†,‡] Vasilii I. Artyukhov,[§] William Regan,[†,‡] Yuanyue Liu,[§] M. F. Crommie,[†,‡] Boris I. Yakobson,*[,§] and A. Zettl*[,†,‡]

[†]Department of Physics and Center of Integrated Nanomechanical Systems, University of California at Berkeley, Berkeley, California 94720, United States

[‡]Materials Sciences Division, Lawrence Berkeley National Laboratory, Berkeley, California 94720, United States

[§]Department of Mechanical Engineering and Materials Science, Department of Chemistry, and the Richard E. Smalley Institute for Nanoscale Science and Technology, Rice University, Houston, Texas 77005, United States

S *Supporting Information*

ABSTRACT: The understanding of crack formation due to applied stress is key to predicting the ultimate mechanical behavior of many solids. Here we present experimental and theoretical studies on cracks or tears in suspended monolayer graphene membranes. Using transmission electron microscopy, we investigate the crystallographic orientations of tears. Edges from mechanically induced ripping exhibit straight lines and are predominantly aligned in the armchair or zigzag directions of the graphene lattice. Electron-beam induced propagation of tears is also observed. Theoretical simulations account for the observed preferred tear directions, attributing the observed effect to an unusual nonmonotonic dependence of graphene edge energy on edge orientation with respect to the lattice. Furthermore, we study the behavior of tears in the vicinity of graphene grain boundaries, where tears surprisingly do not follow but cross grain boundaries. Our study provides significant insights into breakdown mechanisms of graphene in the presence of defective structures such as cracks and grain boundaries.

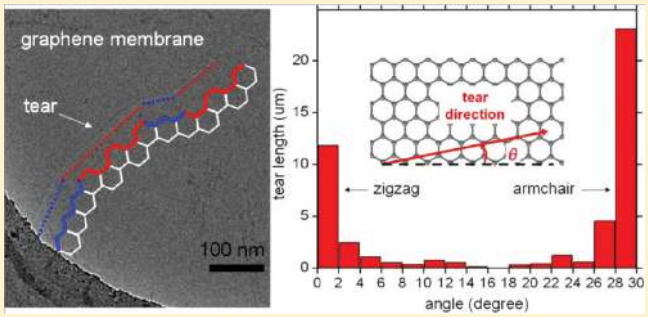

KEYWORDS: *Graphene, crack, tear, crack propagation, graphene edge, grain boundary*

Graphene, a one-atom thick sp^2-bonded carbon membrane, exhibits spectacular electronic and thermal properties.[1,2] The mechanical properties are equally outstanding, with a Young's modulus of around 1 TPa and mechanical strength of more than 100 GPa,[3] which makes graphene a promising candidate for strengthening components in composite materials and for other nanomechanical systems applications.[4−7] Moreover, graphene is flexible in the out-of-plane direction, which is advantageous for applications in flexible transparent electrodes and devices.[8]

In many solids, the formation of cracks due to applied stress is a well-known failure mechanism and hence one of the most important problems in materials science. In a two-dimensional sheetlike material such as graphene, applied tensile stress can also lead to catastrophic failure (ripping) by related crack formation, which we call tearing. The study of tearing in graphene is not only critical in gaining an understanding of the fundamental two-dimensional interatomic interactions, but it has ramifications for a host of mechanical applications (as well as electronic and thermal applications).

Theoretical studies including molecular dynamics simulations have given some insight into the mechanical properties and breakdown mechanisms of graphene under tension.[9−13] Previous experimental studies on graphene's mechanical properties include nanoindentation using atomic force microscopy,[3,14] and an investigation of graphene tearing related to the interaction between graphene and substrates.[15] Most experimental studies, however, have suffered from moderate spatial and time resolution, making it difficult to observe local tear shapes, or their modes of propagations in real time.

In this study, we investigate experimentally and theoretically tears in suspended monolayer graphene. We examine the crystallographic orientations of torn edges using transmission electron microscopy (TEM) imaging and electron diffraction. Torn edges induced by mechanical stress maintain straightness for substantial distances (fractions of micrometers or greater) in either armchair or zigzag direction and occasionally change directions by 30° (or multiples of 30°). We also observe in real time the propagation of tears stimulated by electron beam irradiation. Theoretical simulations that take into account unpaired electrons at torn edges show preferred armchair and zigzag directions for graphene ripping with occasional tear kinks, which is in agreement with experimental observations.

Received: October 9, 2011
Revised: December 9, 2011
Published: December 12, 2011

   dx.doi.org/10.1021/nl203547z | *Nano Lett.* 2012, 12, 293−297

Graphene is obtained by chemical vapor deposition (CVD) on polycrystalline copper.[16] See Supporting Information for detailed methods of sample preparation and experiments. The graphene membrane occasionally develops tears due to unavoidable mechanically applied stress during the graphene transfer process that involves wet etching and drying in air. Figure 1a shows a TEM image of suspended graphene transferred to a TEM grid. The outer circle is the amorphous carbon support boundary for the graphene membrane. A single graphene tear, outlined with a dashed line for clarity, originates from the lower left edge of the carbon support and then extends toward the central region of the membrane. A zoomed-in image around the tear shows that the opening is wider near the carbon support and gets narrower around the tip of the tear, as shown in Figure 1b. This and similar images consistently show that torn edges in graphene are generally straight with occasional changes in direction of 30°, which strongly suggests that the directions of the observed tears are closely related to graphene's hexagonal lattice symmetry.

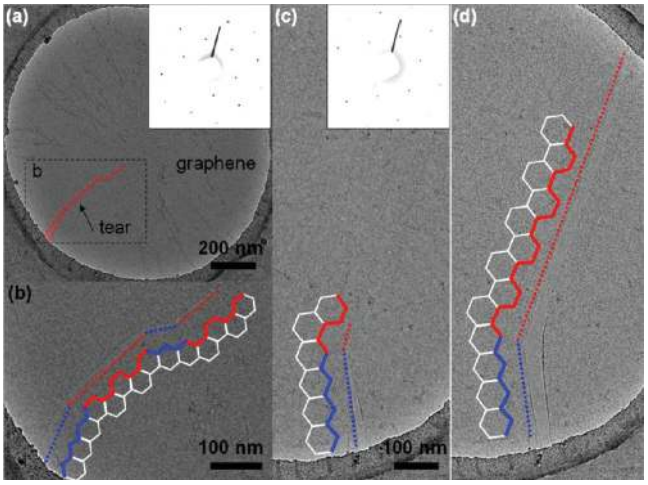

Figure 1. Tears in a suspended graphene membrane. (a) TEM image of suspended graphene transferred to a Quantifoil holey carbon TEM grid with a tear near the edge of the carbon support. The inset is the rotation-calibrated diffraction pattern of graphene. The dashed rectangle is the field of view for panel b. (b) Zoomed-in TEM image of the tear in graphene. The tear exhibits straight lines with the direction occasionally changing by 30°. The red and blue dotted lines represent armchair and zigzag tear edges, respectively. (c) TEM image of a graphene tear before the propagation. The inset is the rotation-calibrated diffraction pattern of graphene membrane. (d) Propagated tear in graphene under the electron beam. The freshly torn line is straight following the armchair direction of the graphene lattice.

To investigate the crystalline directions of torn graphene edges, we perform electron diffraction near tear regions. We note that within the 1.2 μm diameter circular suspended membrane region the samples are typically single-crystal (see below for behavior near grain boundaries).[17] The inset of Figure 1a shows the rotation-calibrated diffraction pattern of graphene for the associated membrane. From the diffraction pattern, we can assign the crystalline direction of the graphene lattice as shown in Figure 1b. We find that the torn edges are aligned with either armchair or zigzag directions. The red and blue dotted lines in Figure 1b represent armchair and zigzag edges in the tear line, respectively. Similar analysis of tears in different suspended graphene membranes consistently show that tears are straight along either the armchair or zigzag directions and occasionally change directions in multiples of 30°.

Tears are found both spanning the entire membrane or only part of the membrane (as in Figure 1a–c). We find that partially spanning tears can sometimes be induced to propagate further by action of the TEM electron beam. Figure 1c,d shows the same area of graphene before and after illumination by the electron beam. The tear maintains its straightness as it grows from its tip. In Figure 1d, the freshly torn edge follows the armchair direction of graphene lattice. The propagation of tears can occur quite fast (up to ~1 μm/sec) with even low electron dosages (~ 0.01 A/cm^2). Previous TEM studies, including atomic resolution TEM work on graphene, provide possible explanations to the mechanisms of observed tear propagation under the electron beam.[18−20] Electron-beam irradiation effects can be categorized into elastic scattering effect (knock-on damage) and inelastic scattering that produces electronic excitations.[21,22] Among these, knock-on damage is generally believed to be the main irradiation effect in graphene since excitation effects are rapidly quenched as a result of metallic nature of graphene.[21] For pristine graphene, the knock-on energy threshold for incident electrons is around 86 keV.[23] We mainly use an electron energy of 100 keV for TEM imaging in this study; however, tear propagation has been observed at lower electron accelerating voltages, including 80 and even 20 kV. Moreover, the rate of tear propagation seems to be enhanced at 20 kV, which does not agree with what we might expect from knock-on irradiation effects.[21] These facts demonstrate that knock-on damage is not the main mechanism of tear propagation.

High-energy electrons can excite the electronic states in graphene by inelastic scattering and breaking bonds locally through ionization damage.[21,22] The effects of ionization damage will be especially dramatic at highly strained and therefore vulnerable carbon−carbon bonds. We believe that the observed tear propagation is mainly caused by a combination of local high strain concentrated at tear tips and ionization effects; high-energy electrons transfer energy to strained carbon−carbon bonds and induce tear propagation. Electron-beam induced heating is another potential contributor to tear propagation (since the negative coefficient of thermal expansion of graphene[24] would increase the tensile strain with heating and thus promote tearing), but given our experimental parameters and graphene's high thermal conductivity,[2] we find that heating is not significant during the imaging.[25] We also note that perfect graphene membranes without preexisting tears exhibit no induced tears under even much higher electron dosages.

Figure 2 shows the crystalline direction-dependent histograms of torn edges. Here we define 0° as along the zigzag direction of tear lines. For statistical significance, we investigate more than 50 partially torn graphene membranes. As expected, a preponderance of the tear lines is aligned with either the armchair or zigzag direction. Interestingly, armchair direction tear lines are twice as prominent as those in the zigzag direction.

We now turn to a theoretical analysis of tearing in graphene. We first note that the prevalence of tear lines in armchair and zigzag directions and abrupt angle changes between these directions are not obvious from simple classical fracture theory.[26] The strength to crack propagation is measured by the critical stress intensity factor $K \sim (Y\gamma)^{1/2}$, where Y is Young's modulus and γ is surface energy, or edge energy in case

dx.doi.org/10.1021/nl203547z | Nano Lett. 2012, 12, 293−297

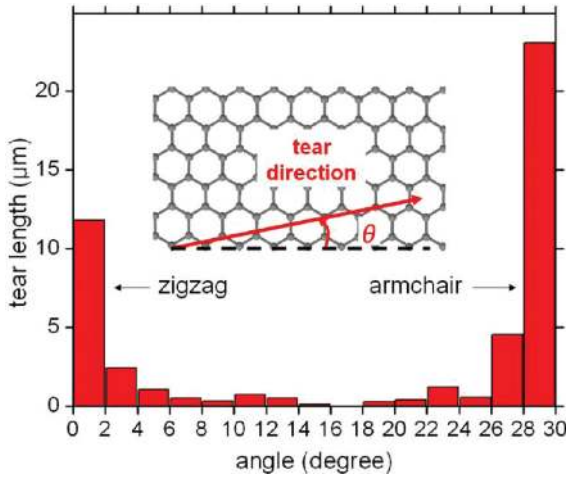

Figure 2. Histograms of angle dependence in torn edges. The 0° is defined as the zigzag direction of the graphene lattice (Inset). Most tear lines align to either the armchair or zigzag direction. Armchair-aligned tear lines are about twice as abundant as zigzag.

of graphene. Since Y is isotropic for graphene, critical stress will be mainly determined by the edge energy γ. Our observations imply that the angle-dependent energy curve for graphene edge is a concave function with minima at 0 and 30°, an unusual trend.[27]

Consider a graphene sheet under strain applied at an angle χ to the armchair direction of graphene. The inset in Figure 3

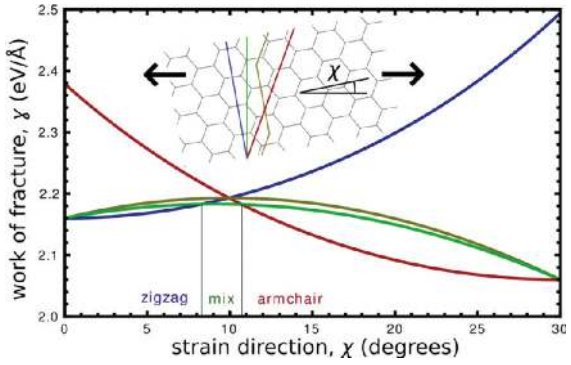

Figure 3. Direction-dependent energetics of cracks in graphene. At a given orientation of local strain with respect to graphene lattice, as described by the angle χ, the lowest-energy curve represents the stable crack direction. The intermediate direction of edge (green) is favorable only in a narrow window of χ, so that armchair and zigzag-edged tears should be observed predominantly.

shows possible crack paths in this situation: (green) shortest path normal to the applied strain with an intermediate orientation of the crack; (red and blue) along pure armchair or zigzag directions at an acute angle to the strain direction; or (olive) a piecewise-straight crack composed of long pure zigzag and armchair segments such that on average it remains normal to the strain. The plot in Figure 3 shows the dependence of energy of each crack type on the orientation of strain using the analytical expressions for edge energies[27] and numerical data calculated using the ReaxFF forcefield.[28,29] At each given angle χ, our model predicts the lowest-lying curve to represent the energetically preferred crack direction. It can be seen that there exists only a narrow interval of orientations at which intermediate-direction cracks are favored, and under realistic conditions of inhomogeneous local strain distribution that also changes as the crack propagates, only straight armchair or zigzag crack edges should be seen.

To verify the predictions of this energetic argument, we simulate ripping graphene under tension using the same forcefield. We take rectangular graphene sheets with a tear tip placed at the right edge (marked with yellow arrows) as shown in Figure 4a–c. The graphene lattice is oriented with the

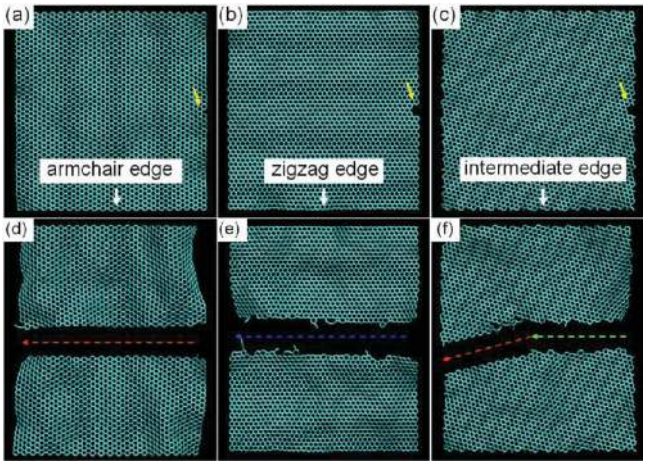

Figure 4. Simulations of ripping graphene. (a–c) Rectangular graphene sheet seeded with a tear tip at the right side (marked with yellow arrows). In the horizontal direction, the edges of graphene show (a) armchair, (b) zigzag and (c) intermediate edges, respectively. Tension is applied vertically and induces the propagation of the tears from right to left in the simulation. (d–f) Simulation results after the tear propagations. (d,e) The torn edges maintain straightness in the armchair (red dashed lines) or zigzag (blue dashed line) directions. (f) For the intermediate direction, the tear edge initially follows the horizontal direction (green) but then changes direction and follows the armchair edge direction. (Animated trajectories are available as Supporting Information Movie 1).

horizontal along an (a) armchair, (b) zigzag, and (c) intermediate edge, respectively. Tension is applied vertically and induces the propagation of the tears from right to left in the simulation (see also Supporting Information Movie S1). Figure 4d–f shows final results after the tear propagations. The torn edges maintain straightness in the armchair (red dashed lines) or zigzag (blue dashed line) directions as shown in Figure 4d,e. As predicted above, for the intermediate direction the tear edge follows the horizontal direction in the beginning but changes its direction to follow the armchair edge direction, thus minimizing crack energy despite increasing its length (Figure 4f). These simulation results agree very well with our experimental observations. We also note that torn edges, especially in the armchair direction, exhibit atomically clean edge structures. Intentionally tearing graphene may thus be a good way to obtain graphene nanoribbons with atomically well-define edges.

Supporting Information Movies S2 and S3 show molecular dynamics simulations of graphene tearing under more complex strain, as the sheets are pulled by two adjacent corners. In this setup, strain direction at the crack tip changes significantly over time. However, we still observe mostly piecewise-straight armchair or zigzag crack edges making sharp turns.

Also of interest is the behavior of tears in the vicinity of, or even crossing, structural anomalies such as folds or grain

dx.doi.org/10.1021/nl203547z | Nano Lett. 2012, 12, 293–297

boundaries (GBs). Although our suspended membranes are mostly defect-free, on occasion folds[30] or GBs[17,31] will cross the sample, as our CVD graphene exhibits tilt grains of size with a few to tens of micrometers.[17] Previous studies suggest that the presence of a GB may have detrimental effects on the mechanical strength of the graphene membrane.[14,31,32] In our experiments, graphene GBs are readily identified with observations of adsorbents along the GBs and diffraction analysis.[17,31] Interestingly, we find that in cases where GBs do exist within the suspended membrane, the observed tears do not generally coincide with GBs, and the same crystalline orientation is seen on the two opposing sides of a tear line. Invariably we observe tear lines following the usual armchair or zigzag directions in the graphene lattice that may happen to cross a GB with minimal perturbation, as shown in Figure 5.

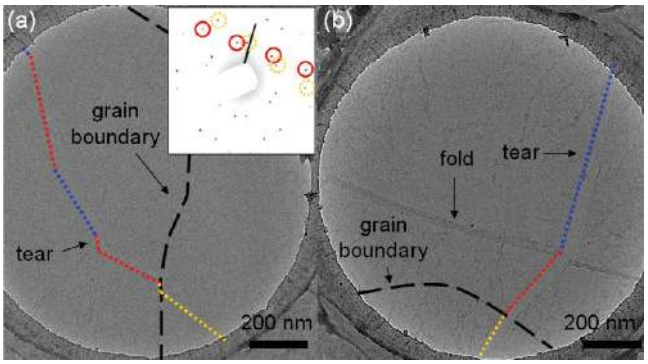

Figure 5. Graphene tears crossing grain boundaries (GBs). (a) TEM image of graphene tear crossing, not following, a grain boundary (GB) in graphene. The GBs are identified by the high absorbent concentration along the grain boundary together with electron diffraction. Inset of the diffraction pattern around the GB showing two sets of hexagonal patterns from two adjacent tilt grains, where the hexagonal pattern marked with red and dashed yellow circles corresponds to the grain in the left and right sides, respectively. The blue dotted lines represent tear lines in the zigzag direction. The red and yellow dotted lines represent tear lines in the armchair direction. (b) Another TEM image of a graphene tear crossing a GB and fold in graphene. The blue dotted line represents a line in the zigzag direction. The red and yellow dotted lines represent the armchair direction.

The observation that tears cross GBs instead of following them appears to contradict the common-knowledge notion that GBs represent "weak spots" of materials. The apparent disagreement originates from the fact that in ductile materials, GBs prevent the migration of defects which is responsible for plastic flow, thus making the material less ductile and easier to break. However, at relevant experimental temperatures (and time scales), sp^2 carbon is expected to behave as a completely brittle material,[33] making this phenomenon irrelevant. GBs in graphene do contain dislocations that produce strain, but the strain fields of consecutive 5−7 pairs actually cancel out locally.[34] From the viewpoint of edge energy analysis, it is important that graphene GBs typically have some random orientation, not coinciding with either AC or ZZ direction. Hence, if the material were to break along the GB, this would expose an energetically unfavorable edge.

At this point, it is worth recalling that K_c also depends on the stiffness of the material, which becomes direction-dependent in the vicinity of a GB. Specifically, it decreases for loads normal to the boundary, which can make nonpristine edges stable. Therefore, the behavior of cracks near grain boundaries can be expected to be bimodal: when the stress is normal to the GB, as is in the case of, for example, recent experiments where AFM tips were indented into the middle of a grain,[14,31] the tear can follow the boundary. However, if the tear initiated away from the GB and at some random orientation with respect to it (so that the strain direction is away from normal to the GB), the stiffness it experiences is more or less unaffected by the GB, and the tear will pass right through it, simply switching to the most favorable direction in the new grain, as is indeed observed in the present work.

In conclusion, we have shown that tears in suspended monolayer graphene predominantly align to the armchair or zigzag directions. Real-time tear propagation has been observed under an electron beam, which is mainly attributed to a combination of high strain at the tip of tears and ionization effects from high-energy electrons. Our theoretical analysis based on the analytical expression for direction-dependent edge energy explains why tears predominantly form along armchair and zigzag directions, and molecular dynamics simulations confirm this explanation. Electron-beam assisted ripping graphene may be an effective and simple way to selectively tailor graphene edges. The edge structures of graphene have important effects on the electronic properties.[35] Controlling the edge structure of graphene, therefore, is of very importance for graphene electronic applications. Our demonstration of tear propagation in graphene via electron beam may be an interesting way to manipulate graphene membranes and allow for selective edge termination.

■ ASSOCIATED CONTENT

Supporting Information

Methods for sample preparation, experiments, simulations, and Supporting Movies S1−3 (molecular dynamics simulations of graphene tearing under tension). This material is available free of charge via the Internet at http://pubs.acs.org.

■ AUTHOR INFORMATION

Corresponding Author

*E-mail: biy@rice.edu (B.I.Y.); azettl@berkeley.edu (A.Z.).

■ ACKNOWLEDGMENTS

This research was supported in part by the Director, Office of Energy Research, Materials Sciences and Engineering Division, of the U.S. Department of Energy under Contract No. DE-AC02-05CH11231, which provided for TEM characterizations; by the National Science Foundation within the Center of Integrated Nanomechanical Systems under Grant EEC-0832819, which provided for CVD graphene synthesis; by the National Science Foundation under Grant 0906539, which provided for suspended sample preparation; and by the Office of Naval Research (MURI), which provided for the design of the experiment. W.R. acknowledges support through a National Science Foundation Graduate Research Fellowship. Work at Rice was supported by the Office of Naval Research (MURI) and by the Lockheed Martin Corporation (LANCER).

■ REFERENCES

(1) Castro Neto, A. H.; Guinea, F.; Peres, N. M. R.; Novoselov, K. S.; Geim, A. K. *Rev. Mod. Phys.* **2009**, *81*, 109−162.

(2) Balandin, A. A.; Ghosh, S.; Bao, W.; Calizo, I.; Teweldebrhan, D.; Miao, F.; Lau, C. N. *Nano Lett.* **2008**, *8*, 902−907.

(3) Lee, C.; Wei, X.; Kysar, J. W.; Hone, J. *Science* **2008**, *321*, 385−388.

(4) Dikin, D. A.; Stankovich, S.; Zimney, E. J.; Piner, R. D.; Dommett, G. H. B.; Evmenenko, G.; Nguyen, S. T.; Ruoff, R. S. *Nature* **2007**, *448*, 457−460.
(5) Rafiee, M. A.; Rafiee, J.; Srivastava, I.; Wang, Z.; Song, H.; Yu, Z.-Z.; Koratkar, N. *Small* **2010**, *6*, 179−183.
(6) Bunch, J. S.; van der Zande, A. M.; Verbridge, S. S.; Frank, I. W.; Tanenbaum, D. M.; Parpia, J. M.; Craighead, H. G.; McEuen, P. L. *Science* **2007**, *315*, 490−493.
(7) Chen, C.; Rosenblatt, S.; Bolotin, K. I.; Kalb, W.; Kim, P.; Kymissis, I.; Stormer, H. L.; Heinz, T. F.; Hone, J. *Nat. Nanotechnol.* **2009**, *4*, 861−867.
(8) Kim, K. S.; Zhao, Y.; Jang, H.; Lee, S. Y.; Kim, J. M.; Kim, K. S.; Ahn, J. H.; Kim, P.; Choi, J. Y.; Hong, B. H. *Nature* **2009**, *457*, 706−710.
(9) Liu, F.; Ming, P.; Li, J. *Phys. Rev. B* **2007**, *76*, 064120.
(10) Omeltchenko, A.; Yu, J.; Kalia, R. K.; Vashishta, P. *Phys. Rev. Lett.* **1997**, *78*, 2148−2151.
(11) Zhao, H.; Min, K.; Aluru, N. R. *Nano Lett.* **2009**, *9*, 3012−3015.
(12) Xu, Z. *J. Comp. Theor. Nanosci.* **2009**, *6*, 625−628.
(13) Terdalkar, S. S.; Huang, S.; Yuan, H.; Rencis, J. J.; Zhu, T.; Zhang, S. *Chem. Phys. Lett.* **2010**, *494*, 218−222.
(14) Ruiz-Vargas, C. S.; Zhuang, H. L.; Huang, P. Y.; van der Zande, A. M.; Garg, S.; McEuen, P. L.; Muller, D. A.; Hennig, R. G.; Park, J. *Nano Lett.* **2011**, *11*, 2259−2263.
(15) Sen, D.; Novoselov, K. S.; Reis, P. M.; Buehler, M. J. *Small* **2010**, *6*, 1108−1116.
(16) Li, X.; Cai, W.; An, J.; Kim, S.; Nah, J.; Yang, D.; Piner, R.; Velamakanni, A.; Jung, I.; Tutuc, E.; Banerjee, S. K.; Colombo, L.; Ruoff, R. S. *Science* **2009**, *324*, 1312−1314.
(17) Kim, K.; Lee, Z.; Regan, W.; Kisielowski, C.; Crommie, M. F.; Zettl, A. *ACS Nano* **2011**, *5*, 2142−2146.
(18) Hashimoto, A.; Suenaga, K.; Gloter, A.; Urita, K.; Iijima, S. *Nature* **2004**, *430*, 870−873.
(19) Meyer, J. C.; Kisielowski, C.; Erni, R.; Rossell, M. D.; Crommie, M. F.; Zettl, A. *Nano Lett.* **2008**, *8*, 3582−3586.
(20) Kotakoski, J.; Krasheninnikov, A. V.; Kaiser, U.; Meyer, J. C. *Phys. Rev. Lett.* **2011**, *106*, 105505.
(21) Banhart, F. *Rep. Prog. Phys.* **1999**, *62*, 1181−1221.
(22) Egerton, R. F.; Li, P.; Malac, M. *Micron* **2004**, *35*, 399−409.
(23) Smith, B. W.; Luzzi, D. E. *J. Appl. Phys.* **2001**, *90*, 3509−3515.
(24) Bao, W.; Miao, F.; Chen, Z.; Zhang, H.; Jang, W.; Dames, C.; Lau, C. N. *Nat. Nanotechnol.* **2009**, *4*, 562−566.
(25) Zobelli, A.; Gloter, A.; Ewels, C. P.; Colliex, C. *Phys. Rev. B* **2008**, *77*, 045410.
(26) Griffith, A. A. *Philos. Trans. R. Soc. London, Ser. A* **1921**, *221*, 163−198.
(27) Liu, Y.; Dobrinsky, A.; Yakobson, B. I. *Phys. Rev. Lett.* **2010**, *105*, 235502.
(28) van Duin, A. C. T.; Dasgupta, S.; Lorant, F.; Goddard, W. A. *J. Phys. Chem. A* **2001**, *105*, 9396−9409.
(29) Mueller, J. E.; van Duin, A. C. T.; Goddard, W. A. *J. Phys. Chem. C* **2010**, *114*, 4939−4949.
(30) Kim, K.; Lee, Z.; Malone, B. D.; Chan, K. T.; Alemán, B.; Regan, W.; Gannett, W.; Crommie, M. F.; Cohen, M. L.; Zettl, A. *Phys. Rev. B* **2011**, *83*, 245433.
(31) Huang, P. Y.; Ruiz-Vargas, C. S.; van der Zande, A. M.; Whitney, W. S.; Levendorf, M. P.; Kevek, J. W.; Garg, S.; Alden, J. S.; Hustedt, C. J.; Zhu, Y.; Park, J.; McEuen, P. L.; Muller, D. A. *Nature* **2011**, *469*, 389−392.
(32) Grantab, R.; Shenoy, V. B.; Ruoff, R. S. *Science* **2010**, *330*, 946−948.
(33) Dumitrica, T.; Hua, M.; Yakobson, B. *Proc. Natl. Acad. Sci. U.S.A.* **2006**, *103*, 6105−6109.
(34) Yakobson, B. I.; Ding, F. *ACS Nano* **2011**, *5*, 1569−1574.
(35) Ritter, K. A.; Lyding, J. W. *Nat. Mater.* **2009**, *8*, 235−242.